Analysis of Feynman scaling of Photon and Neutron Production in the Very Forward Direction in Deep-Inelastic Scattering at HERA

Abstract

Measurements of normalised cross sections for the production of photons and neutrons at very small angles with respect to the proton beam direction as a function of Feynman-x in deep-inelastic positron-proton scattering at HERA are presented. The data are taken with the H1 detector in the years 2006 and 2007 and correspond to an integrated luminosity of $126~\mathrm{pb}^{-1}$. The analysis covers the range of negative four momentum transfer squared at the positron vertex $6 < Q^2 < 100~\mathrm{GeV}^2$, inelasticity $0.05 < y < 0.6$ and the centre-of-mass energy of the virtual photon-proton system $70 < W < 245~\mathrm{GeV}$. The dependence of cross sections on W is investigated. The cross sections are compared to the predictions of DIS models and models of the hadronic interactions of high energy cosmic rays.

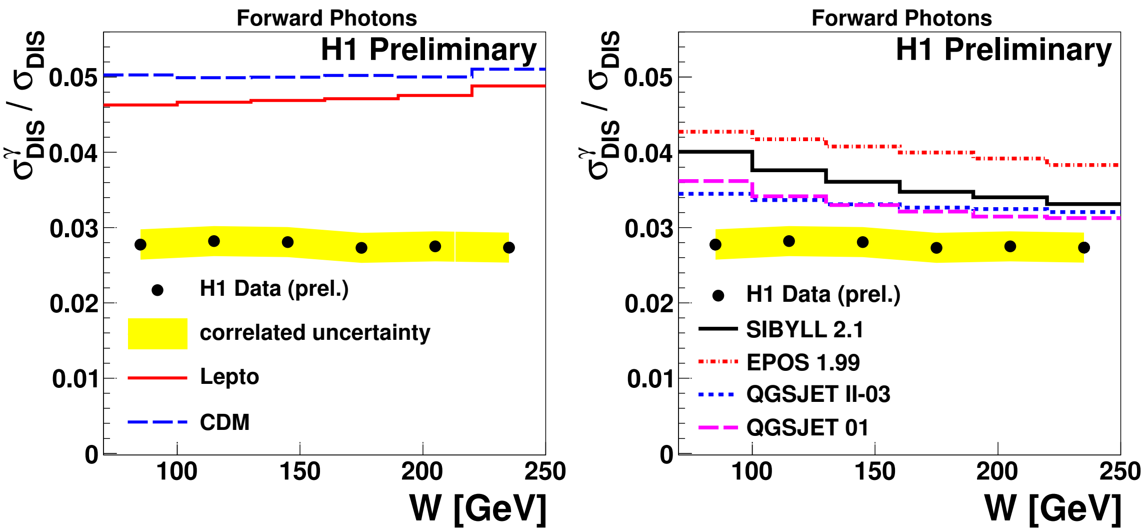

Figure 1: The fraction of DIS events with forward photons in the kinematic region $6 < Q^2 < 100$ GeV^2 and $0.05 < y < 0.6$ and the pseudorapidity of the photon $\eta > 7.9$. as a function of W. The predictions of MC models are compared to the measurements.

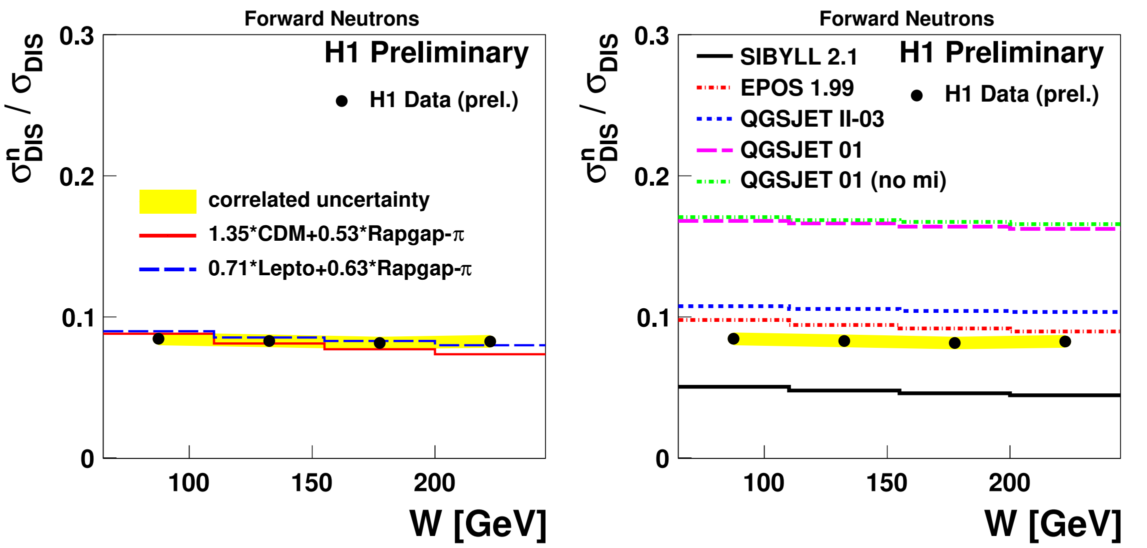

Figure 2: The fraction of DIS events with forward neutrons in the kinematic region $6 < Q^2 < 100$ GeV^2 and $0.05 < y < 0.6$ and the pseudorapidity of the photon $\eta > 7.9$. as a function of W. The predictions of MC models are compared to the measurements.

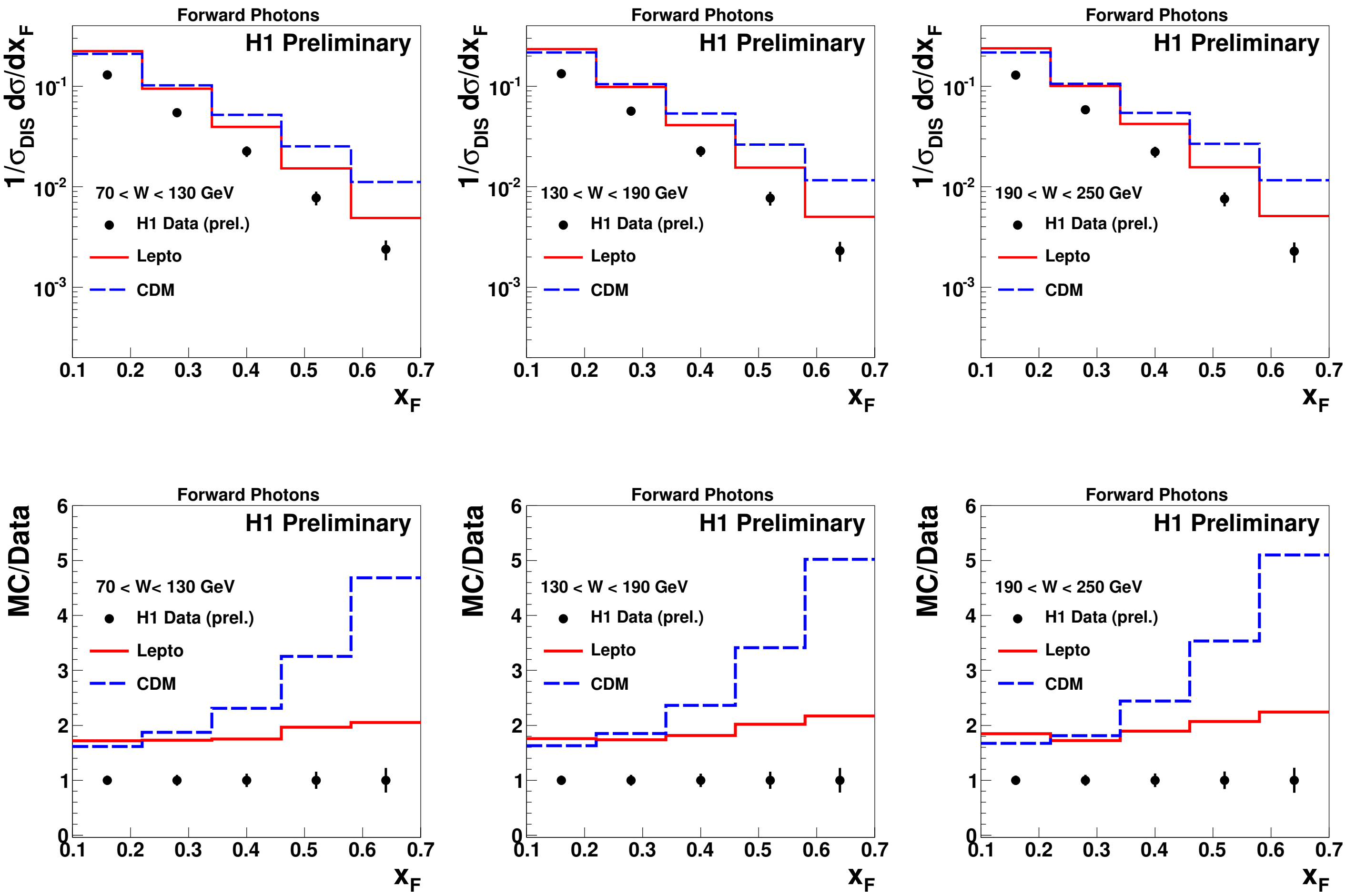

Figure 3: Normalised cross sections of forward photons production in DIS as a function of x_F in the region $\eta > 7.9$, $6 < Q^2 < 100$ GeV^2 and $0.05 < y < 0.6$, and in three W intervals. The data are compared to two predictions of the DJANGOH Monte Carlo simulation, using LEPTO and CDM to simulate higher orders. The lower row shows the ratios of the MC predictions to the data. The error bars show the total experimental uncertainty, defined as the quadratic sum of the statistical and systematic uncertainties.

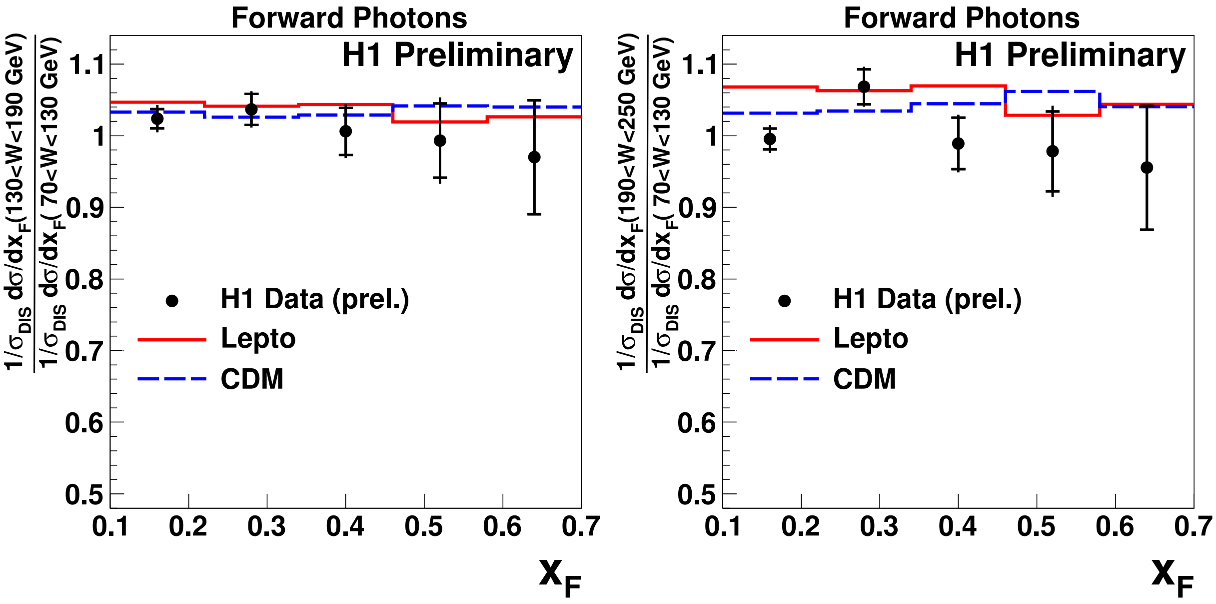

Figure 4: Ratios of normalised cross sections of forward photons production in DIS corresponding to two different W intervals, shown in Fig.2, as a function of x_F. The left side figure shows the ratio of the cross section in $130 < W < 190$ GeV interval to the cross section at $70 < W < 130$ GeV interval. The right side figure shows the ratio of the cross section in $190 < W < 250$ GeV interval to the cross section at $70 < W < 130$ GeV interval. Predictions of LEPTO and CDM MC models are compared to the measurement.

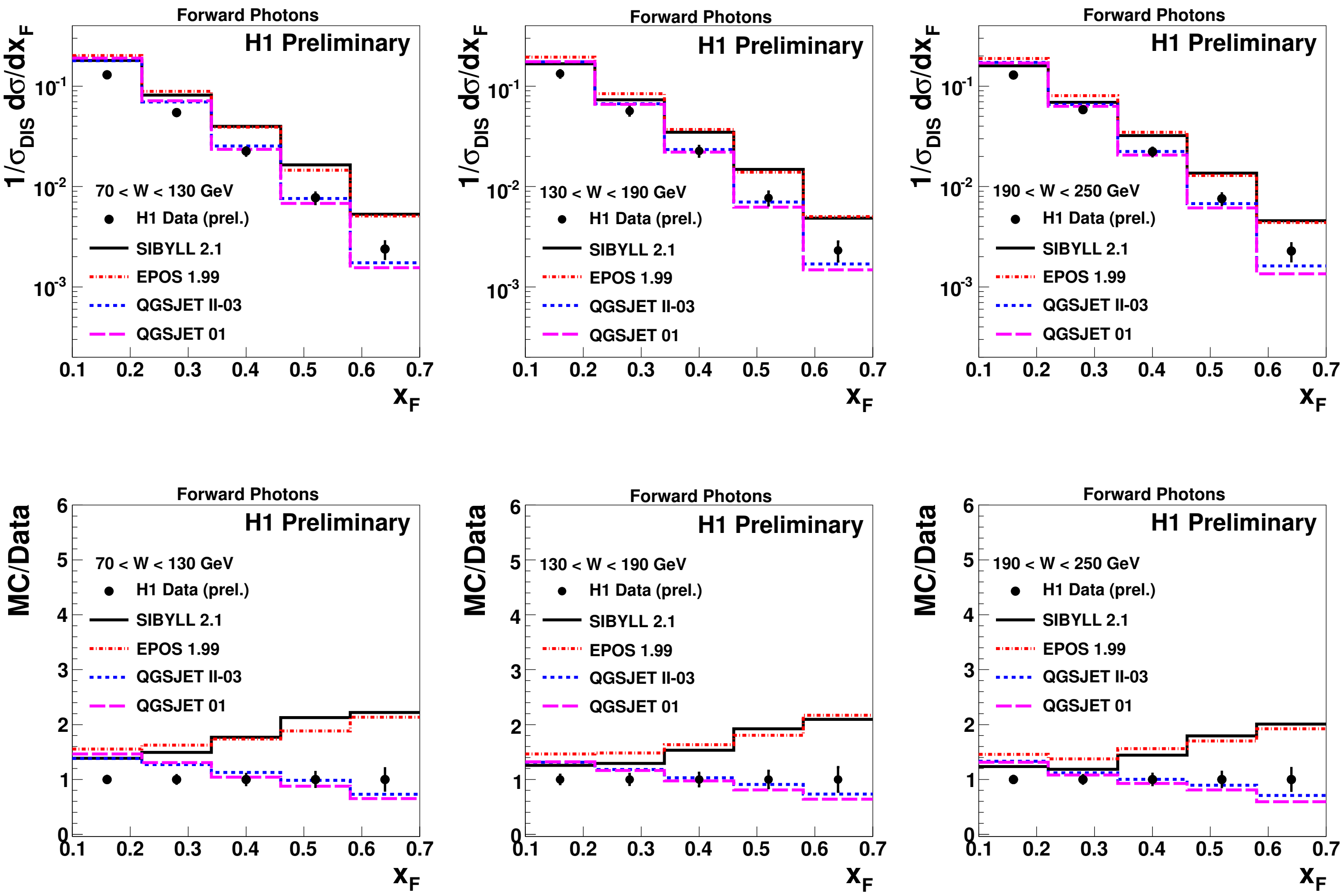

Figure 5: Normalised cross sections of forward photons production in DIS as a function of x_F in the region $\eta > 7.9$, $6 < Q^2 < 100$ GeV^2 and $0.05 < y < 0.6$, and in three W intervals. The data are compared to predictions os hadronic interactions, QGSJET, EPOS and SIBYLL. The lower row shows the ratios of the MC predictions to the data. The error bars show the total experimental uncertainty, defined as the quadratic sum of the statistical and systematic uncertainties.

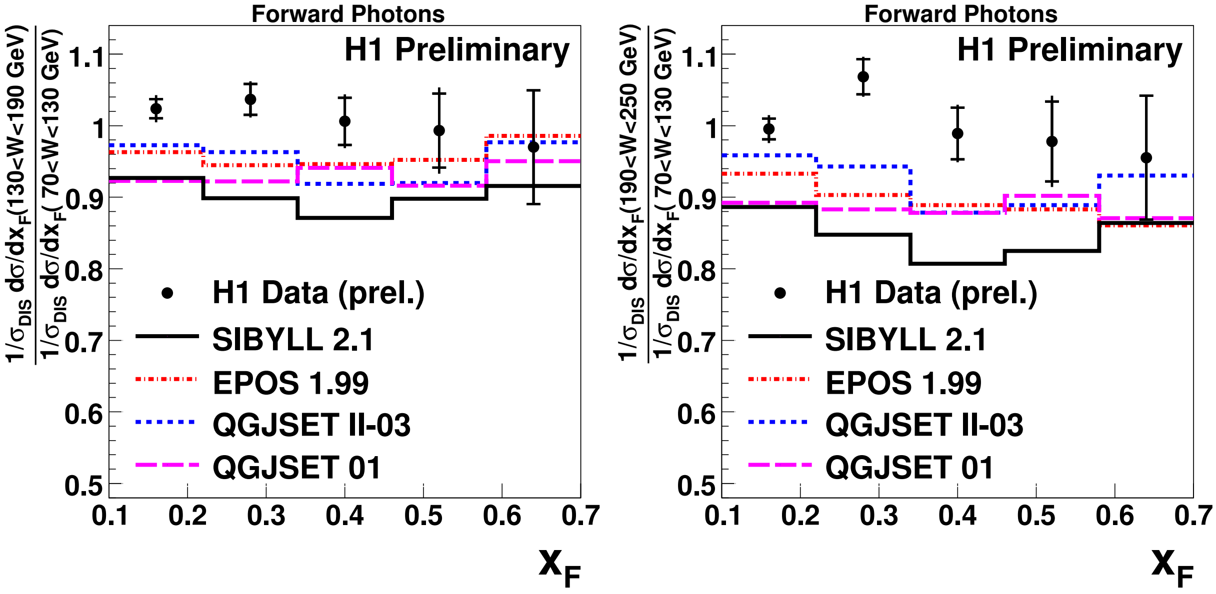

Figure 6: Ratios of normalised cross sections of forward photons production in DIS corresponding to two different W intervals, shown in Fig.4, as a function of x_F. The left side figure shows the ratio of the cross section in $130 < W < 190$ GeV interval to the cross section at $70 < W < 130$ GeV interval. The right side figure shows the ratio of the cross section in $190 < W < 250$ GeV interval to the cross section at $70 < W < 130$ GeV interval. Predictions of LEPTO and CDM MC models are compared to the measurement. Predictions of CR models are compared to the measurement.

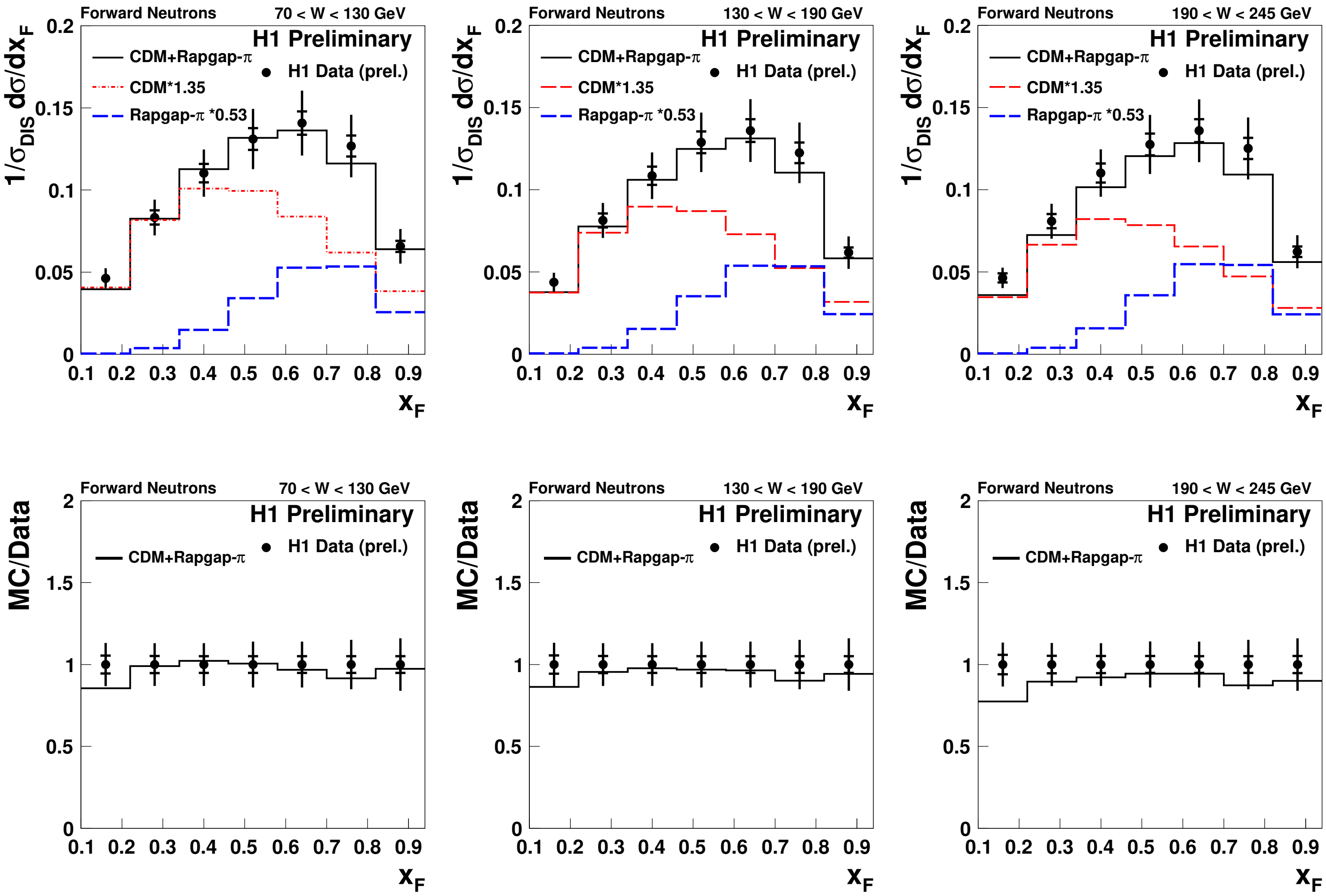

Figure 7: Normalised cross sections of forward neutron production in DIS as a function of x_F in the region $\eta > 7.9$, $6 < Q^2 < 100$ GeV^2 and $0.05 < y < 0.6$, and in three W intervals. The data are compared to two predictions of the Monte Carlo simulations CDM (Djangoh) and RAPGAP-π, and the combination of CDM and RAPGAP-π, multipled by the normalisation factors. The lower row shows the ratios of the MC predictions to the data. The error bars show the total experimental uncertainty, defined as the quadratic sum of the statistical and systematic uncertainties.

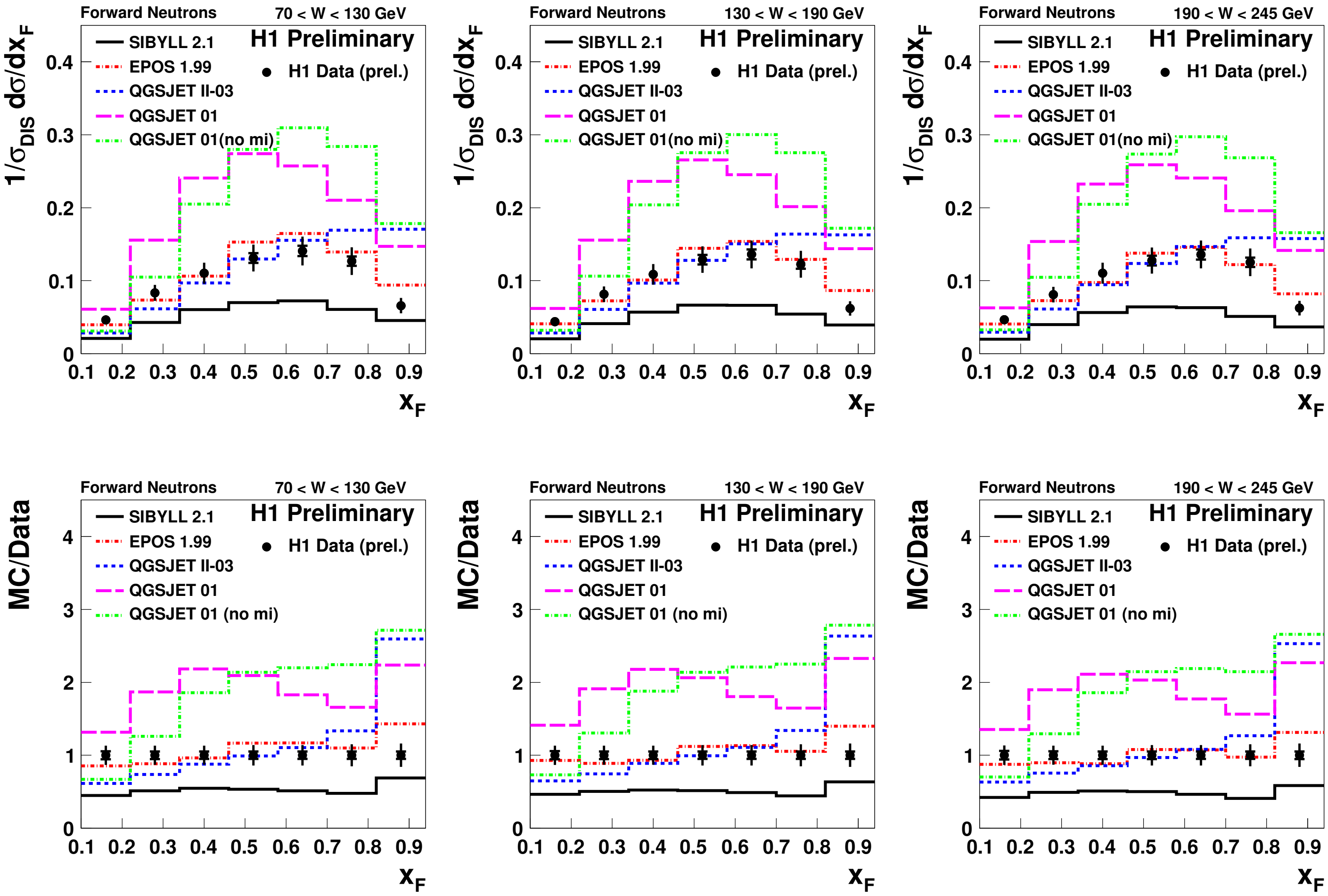

Figure 8: Normalised cross sections of forward neutron production in DIS as a function of x_F in the region $\eta > 7.9$, $6 < Q^2 < 100$ GeV^2 and $0.05 < y < 0.6$, and in three W intervals. The data are compared to predictions os hadronic interactions, QGSJET, EPOS and SIBYLL. The lower row shows the ratios of the MC predictions to the data. The error bars show the total experimental uncertainty, defined as the quadratic sum of the statistical and systematic uncertainties.

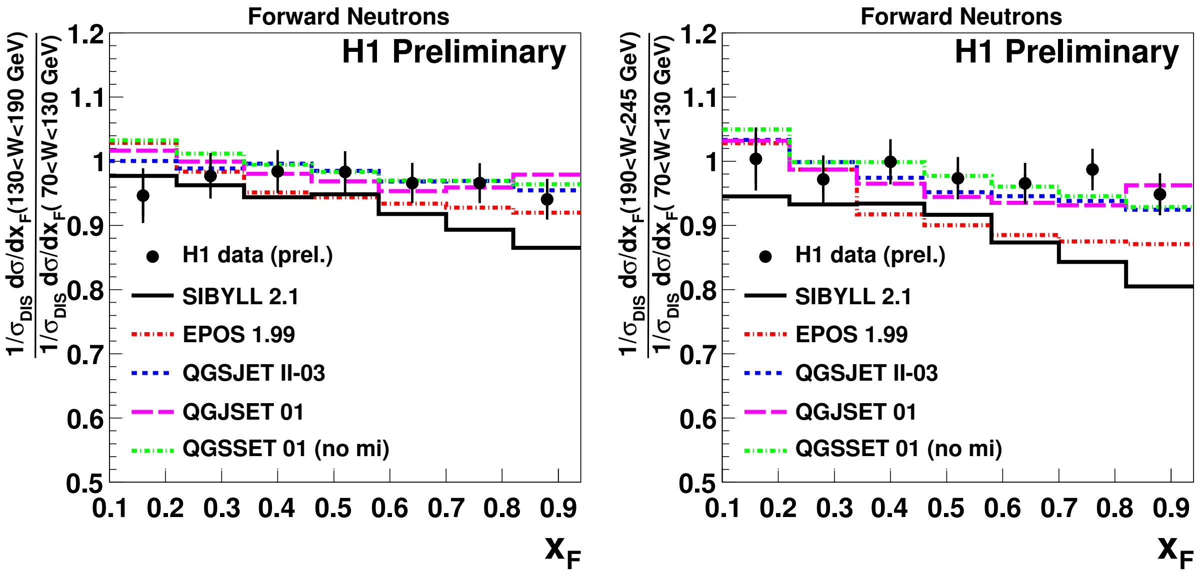

Figure 9: Ratios of normalised cross sections of forward neutron production in DIS corresponding to two different W intervals, shown in Fig.8, as a function of x_F. The left side figure shows the ratio of the cross section in $130 < W < 190$ GeV interval to the cross section at $70 < W < 130$ GeV interval. The right side figure shows the ratio of the cross section in $190 < W < 245$ GeV interval to the cross section at $70 < W < 130$ GeV interval. Predictions of CR models are compared to the measurement.